Investigation of blue emission from Raman-active crystals: Its origin and impact on laser performance

Jonas Jakutis Neto,[1, 2, *] Christopher Artlett,[1] Andrew Lee,[1] Jipeng Lin,[1] David Spence,[1] James Piper,[1] Niklaus Ursus Wetter[2] and Helen Pask[1]

[1]*MQ Photonics Research Centre, Department of Physics, Macquarie University, Sydney, NSW 2109, Australia*
[2]*Instituto de Pesquisas Energéticas e Nucleares, CNEN/SP, Universidade de São Paulo, CEP 05508-000, São Paulo/SP, Brazil*
[*]*jonasjakutis@usp.br*

Abstract: The origin and consequences to laser performance of blue emission observed in some Raman crystals has been studied in detail, leading us to attribute the origin of the phenomenon to fluorescence from $Tm^{3+}(^1G_4)$ impurity ions which are excited via sequential upconversion. For the specific case of a Nd:YLF/KGW Raman laser, we show that the blue fluorescence has modest but significant impacts on laser performance and thermal loading. If the blue fluorescence was eliminated, then laser efficiency could be increased by 15% and thermal loading in the KGW crystal reduced by 17%.

OCIS codes: (140.3550) Lasers, Raman; (140.3580) Lasers, solid-state; (140.5680) Rare earth and transition metal solid-state lasers.

References and links

1. A. S. Grabtchikov, A. N. Kuzmin, V. A. Lisinetskii, G. I. Ryabtsev, V. A. Orlovich, and A. A. Demidovich, "Stimulated Raman scattering in Nd:KGW laser with diode pumping," J. Alloy. Comp. **300–301**(0), 300–302 (2000).
2. H. M. Pask, "Continuous-wave, all-solid-state, intracavity Raman laser," Opt. Lett. **30**(18), 2454–2456 (2005).
3. L. Fan, Y. X. Fan, Y. Q. Li, H. Zhang, Q. Wang, J. Wang, and H. T. Wang, "High-efficiency continuous-wave Raman conversion with a $BaWO_4$ Raman crystal," Opt. Lett. **34**(11), 1687–1689 (2009).
4. A. J. Lee, H. M. Pask, J. A. Piper, H. J. Zhang, and J. Y. Wang, "An intracavity, frequency-doubled $BaWO_4$ Raman laser generating multi-watt continuous-wave, yellow emission," Opt. Express **18**(6), 5984–5992 (2010).
5. Y. M. Duan, H. Y. Zhu, G. Zhang, C. H. Huang, Y. Wei, C. Y. Tu, Z. J. Zhu, F. G. Yang, and Z. Y. You, "Efficient 559.6 nm light produced by sum-frequency generation of diode-end-pumped Nd:YAG/$SrWO_4$ Raman laser," Laser Phys. Lett. **7**(7), 491–494 (2010).
6. Y. Duan, F. Yang, H. Zhu, Z. Zhu, C. Huang, Z. You, Y. Wei, G. Zhang, and C. Tu, "Continuous-wave 560 nm light generated by intracavity $SrWO_4$ Raman and KTP sum-frequency mixing," Opt. Commun. **283**(24), 5135–5138 (2010).
7. H. Y. Zhu, Y. M. Duan, G. Zhang, C. H. Huang, Y. Wei, W. D. Chen, Y. D. Huang, and N. Ye, "Yellow-light generation of 5.7 W by intracavity doubling self-Raman laser of YVO_4/Nd:YVO_4 composite," Opt. Lett. **34**(18), 2763–2765 (2009).
8. W. Baoshan, T. Huiming, P. Jiying, M. Jieguang, and G. Lanlan, "Low threshold, diode end-pumped Nd^{3+}:$GdVO_4$ self-Raman laser," Opt. Mater. **29**(12), 1817–1820 (2007).
9. H. Yu, Z. Li, A. J. Lee, J. Li, H. Zhang, J. Wang, H. M. Pask, J. A. Piper, and M. Jiang, "A continuous wave $SrMoO_4$ Raman laser," Opt. Lett. **36**(4), 579–581 (2011).
10. M. T. Chang, W. Z. Zhuang, K. W. Su, Y. T. Yu, and Y. F. Chen, "Efficient continuous-wave self-Raman Yb:KGW laser with a shift of 89 cm^{-1}," Opt. Express **21**(21), 24590–24598 (2013).
11. A. J. Lee, H. M. Pask, D. J. Spence, and J. A. Piper, "Efficient 5.3 W CW laser at 559 nm by intracavity frequency summation of fundamental and first-Stokes wavelengths in a self-Raman Nd:$GdVO_4$ laser," Opt. Lett. **35**(5), 682–684 (2010).
12. D. J. Spence, X. Li, A. J. Lee, and H. M. Pask, "Modeling of wavelength-selectable visible Raman lasers," Opt. Commun. **285**(18), 3849–3854 (2012).
13. G. M. Bonner, H. M. Pask, A. J. Lee, A. J. Kemp, J. Wang, H. Zhang, and T. Omatsu, "Measurement of thermal lensing in a CW $BaWO_4$ intracavity Raman laser," Opt. Express **20**(9), 9810–9818 (2012).

#203411 - $15.00 USD Received 24 Dec 2013; revised 22 Mar 2014; accepted 27 Mar 2014; published 1 Apr 2014

14. H. Zhu, Y. Duan, G. Zhang, Y. Zhang, and F. Yang, "Laser induced blue luminescence phenomenon," Jpn. J. Appl. Phys. **50** (Copyright (C) 2011 The Japan Society of Applied Physics), 090203 (2011).
15. I. A. Khodasevich, A. A. Kornienko, E. B. Dunina, and A. S. Grabtchikov, "On the influence of dopant ions on blue emission in KGW crystal excited by infrared laser radiation," J. Appl. Spectrosc. **79**(1), 38–45 (2012).
16. I. A. Khodasevich, A. A. Kornienko, E. B. Dunina, and A. S. Grabtchikov, "Transformation of optical properties of crystal media (KGW, YVO_4) exposed to quasi-continuous laser radiation in the range of the transmission band of the medium," Opt. Spectrosc. **115**(3), 325–334 (2013).
17. Y. F. Chen, "Efficient 1521-nm Nd:$GdVO_4$ Raman laser," Opt. Lett. **29**(22), 2632–2634 (2004).
18. N. Zong, Q. J. Cui, Q. L. Ma, X. F. Zhang, Y. F. Lu, C. M. Li, D. F. Cui, Z. Y. Xu, H. J. Zhang, and J. Y. Wang, "High average power 1.5 microm eye-safe Raman shifting in $BaWO_4$ crystals," Appl. Opt. **48**(1), 7–10 (2009).
19. Y. T. Chang, K. W. Su, H. L. Chang, and Y. F. Chen, "Compact efficient Q-switched eye-safe laser at 1525 nm with a double-end diffusion-bonded Nd:YVO_4 crystal as a self-Raman medium," Opt. Express **17**(6), 4330–4335 (2009).
20. R. Lisiecki, W. Ryba-Romanowski, and T. Lukasiewicz, "Blue up-conversion with excitation into Tm ions at 808 nm in YVO_4 crystals co-doped with thulium and ytterbium," Appl. Phys. B **81**(1), 43–47 (2005).
21. F. Güell, X. Mateos, J. Gavaldà, R. Solé, M. Aguiló, D. Amp, F. Díaz, M. Galan, and J. Massons, "Optical characterization of Tm^{3+}-doped $KGd(WO_4)_2$ single crystals," Opt. Mater. **25**(1), 71–77 (2004).
22. F. Güell, X. Mateos, J. Gavaldà, R. Solé, M. Aguiló, D. Amp, F. Díaz, and J. Massons, "Blue luminescence in Tm^{3+}-doped $KGd(WO_4)_2$ single crystals," J. Lumin. **106**(2), 109–114 (2004).
23. Y. Yang, B. Yao, B. Chen, C. Wang, G. Ren, and X. Wang, "Judd–Ofelt analysis of spectroscopic properties of Tm^{3+}, Ho^{3+} doped $GdVO_4$ crystals," Opt. Mater. **29**(9), 1159–1165 (2007).
24. F. S. Ermeneux, C. Goutaudier, R. Moncorgé, M. T. Cohen-Adad, M. Bettinelli, and E. Cavalli, "Growth and fluorescence properties of Tm^{3+} doped YVO_4 and Y_2O_3 single crystals," Opt. Mater. **8**(1–2), 83–90 (1997).
25. K. H. Esbensen, D. Guyot, and F. Westad, *Multivariate Data Analysis: In Practice* (Camo, 2000).
26. A. A. Kaminskii, *Laser Crystals: Their Physics and Properties* (Springer-Verlag, 1981).
27. R. Paschotta, N. Moore, W. A. Clarkson, A. C. Tropper, D. C. Hanna, and G. Maze, "230 mW of blue light from a thulium-doped upconversion fiber laser," IEEE J. Sel. Top. Quantum Electron. **3**(4), 1100–1102 (1997).
28. X. Li, H. M. Pask, A. J. Lee, Y. Huo, J. A. Piper, and D. J. Spence, "Miniature wavelength-selectable Raman laser: new insights for optimizing performance," Opt. Express **19**(25), 25623–25631 (2011).
29. P. Dekker, H. M. Pask, D. J. Spence, and J. A. Piper, "Continuous-wave, intracavity doubled, self-Raman laser operation in Nd:$GdVO_4$ at 586.5 nm," Opt. Express **15**(11), 7038–7046 (2007).
30. T. Omatsu, M. Okida, A. Lee, and H. M. Pask, "Thermal lensing in a diode-end-pumped continuous-wave self-Raman Nd-doped $GdVO_4$ laser," J. Appl. Phys. B **108**(1), 73–79 (2012).

Introduction

Crystalline Raman lasers offer a practical and efficient approach to laser frequency conversion. They have been extensively studied around the world, using a diverse range of Raman active media, configurations, and temporal regimes that include continuous wave (CW), nanosecond pulse and ultrafast pulse. An unusual phenomenon has been observed in many of these lasers, a blue luminescence, and this has become a subject of speculation as to its origin and effect on Raman laser performance. Above the threshold for the stimulated Raman scattering (SRS), such luminescence is strong, clearly visible and bright in a well-lit room. It is isotropic and emanates from the resonator mode volume. Several groups have reported the effect in their Raman lasers, showing the presence of the phenomenon in many different crystals, KGW [1, 2], $BaWO_4$ [3, 4], $SrWO_4$ [5, 6], YVO_4 [7], $GdVO_4$ [8], $LuVO_4$ and $SrMoO_4$ [9], all based in Neodymium lasers. It was also reported in a Yb:KGW laser [10]. Some authors tried to explain the origin of the emission, either by upconversion in Nd^{3+} ions [1, 8], or by upconversion in Tm^{3+} impurity ions [2]. However, the focus of these works was the Raman laser itself, and the blue luminescence was a secondary issue, discussed only briefly.

Raman lasers have now reached a high level of development with simple CW intracavity Raman lasers reaching overall efficiencies of up to 13% [3] in the infrared (IR) and 21% in the visible [11]. It has been shown that minimizing resonator losses [12] and managing the effects of thermal loading [13] are critical to achieving such high performance. A better understanding of the origins of the observed blue luminescence is necessary, so that the potential effects on Raman laser performance, either as an extra loss, or as an extra source of thermal load, can be determined.

#203411 - $15.00 USD Received 24 Dec 2013; revised 22 Mar 2014; accepted 27 Mar 2014; published 1 Apr 2014

Recently, three published articles have specifically discussed the blue luminescence [14–16]. Zhu *et al.* [14] characterized the emission in three crystals, YVO_4, $GdVO_4$ and $SrWO_4$, with fundamental oscillations at 1063 nm, 1064 nm, 1079 nm and 1342 nm. The strongest blue emissions were found in $SrWO_4$ crystals, when the fundamental was in the 1 μm range, but no luminescence was observed for the 1342 nm fundamental. They concluded that the luminescence occurred with only fundamental oscillation at around 1 μm, and in the presence or absence of the SRS process. However, they did not explain the origin of the emission. In [15], Khodasevich *et al.* made a deeper analysis of the phenomenon, comparing the experimental blue emission spectrum from a KGW crystal with calculated lineshapes for Nd:KGW and Tm:YLF crystals. They found more similarities with the Neodymium emission band around 475 nm than with the Thulium band, but concluded there was not enough evidence to state that Nd^{3+} is responsible for the blue emission. They did not however compare to spectra from Tm:KGW, and ultimately concluded that neither Nd^{3+} nor Tm^{3+} impurities were the origin of the emission and that an alternative explanation was needed. Subsequently Khodasevich *et al.* [16], proposed that the blue emission is originated from a transformation, or change of the optical properties of the crystals that results from exposure to intense light for relatively long periods of time.

In this paper, we present a comprehensive spectroscopic study of the blue emission from Raman lasers that goes well beyond the scope of previous studies. We have investigated the spectra, power dependence and lifetimes for the blue emission from several Raman-active crystals, and measured the concentration of impurity ions such as Tm^{3+} in these crystals. Our measurements, which are more extensive but largely consistent with other studies in the literature, show that the blue emission most probably emanates from Tm^{3+} ions which are present as impurities in the crystals we investigated. A three-step upconversion process is proposed for exciting the $Tm^{3+}(^1G_4)$ from which the blue emission emanates. In the second part of the paper we consider the implication of this upconversion process for laser operation, particularly with regard to laser efficiency and thermal loading of the Raman crystal. We find that the upconversion process leading to blue emission results in a modest but significant decrease in laser efficiency and increases in thermal loading.

Part 1: Spectroscopic investigation of the blue emission

1.1 The occurrence of blue luminescence in Raman-active crystals

As noted in the introduction, blue emission has been observed in numerous Raman-active crystals. There are other Raman-active crystals which do not exhibit blue emission. Based on our extensive studies of using a large number of Raman-active crystals over many years, in which the excitation laser for SRS has been a Nd laser operating around 1μm, we can list the crystals in which we have observed blue emission as: $BaWO_4$, $SrMoO_4$, $KGd(WO_4)_2$ (KGW), Nd:KGW, YVO_4, Nd:YVO_4, Nd:$GdVO_4$, and $LuVO_4$. Those Raman-active crystals in which we have observed an absence of blue emission include: $Ba(NO_3)_2$, $LiIO_3$, diamond, KTP and $LiNbO_3$. We have found no reports in the literature of blue emission from Raman lasers pumped at 1.3 μm and generating first Stokes emission around 1.5 μm [17–19], in contrast to the case of Raman lasers based on the 1.06 μm transition where reports of blue fluorescence are prolific. Figure 1(a) is a photograph showing strong blue light emanating isotropically from the region of a KGW crystal which overlaps the resonator modes. Below the threshold for SRS, the blue emission is weak but visible. In [14], the research was focused on the blue emission excited by the fundamental wavelength around 1 μm only, while this work, like [16], focuses on the much stronger blue emission that occurs in the presence of SRS process. Figure 1(b) shows the blue emission as a function of diode pump power, together with a much weaker red emission that typically accompanies the blue emission, also reported in [10]. It is clear that their intensities are considerably higher when above the threshold for SRS, in this case around 4 W. The same observation was made in [16]. In this work we also observed the

#203411 - $15.00 USD Received 24 Dec 2013; revised 22 Mar 2014; accepted 27 Mar 2014; published 1 Apr 2014

blue emission for an acousto-optic Q-switched laser, and found it to be much weaker than for the CW case. This was consistent with the low duty cycle (<0.1%) of the Q-switched laser. Finally, we note that for Raman lasers with separate laser gain and Raman crystals, any blue emission in the laser crystal was much weaker than in the Raman crystal, indeed in most cases it was not observable by eye.

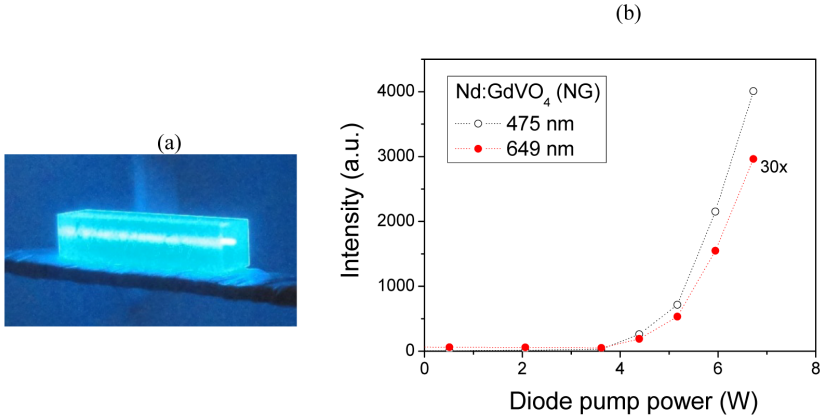

Fig. 1. (a) Picture of the blue emission in a 25mm long KGW crystal and (b) curve showing the intensity of the blue and red (30x) luminescence as a function of diode pump power for a Nd:$GdVO_4$ crystal from Northrop Grumman (NG)

1.2 The spectral properties and lifetime of the blue luminescence

We investigated several Raman-active crystalline media from which blue emission has been previously reported. Specifically we studied KGW (EKSMA), $BaWO_4$ (State Key Laboratory of Crystal Materials, Shandong University, China), 0.3% Nd:$GdVO_4$ (from Castech and Northrop Grumman), YVO_4 (Castech) and 0.5% Nd:YVO_4 (FEE). In each case, a portion of the blue emission exiting the crystal face was coupled into a fiber with a 200 μm diameter by means of two spherical lenses, and was analysed using an spectrometer (Ocean Optics HR4000) which had a resolution of 0.1 nm. The Raman laser cavity for the self-Raman cases comprised a flat mirror (M1) as the pump mirror, with high reflectivity (HR) at 1064 nm and 1177 nm (R>99.9%) and a plane-concave mirror (M2) with radius of curvature (ROC) of 200 mm as the output coupler, either with HR coatings at both 1064 nm and 1177 nm (R>99.9%) or with 0.4% transmission at 1177 nm to couple out the 1st Stokes. The laser cavity was typically 50 mm long, providing a resonator mode in the laser crystal of around 340 μm in diameter that was well matched to the diode pump beam. Nd:$GdVO_4$ and Nd:YVO_4 were investigated using a self-Raman configuration (i.e. these crystals perform the dual functions of generating the fundamental and SRS). For the other crystals, a separate Raman crystal was used as depicted in Fig. 2. The cavity elements and length were changed to maintain similar beam parameters in the laser crystal. A 30 W fiber-coupled diode laser emitting at 880 nm was used to pump the Nd doped crystals.

#203411 - $15.00 USD Received 24 Dec 2013; revised 22 Mar 2014; accepted 27 Mar 2014; published 1 Apr 2014

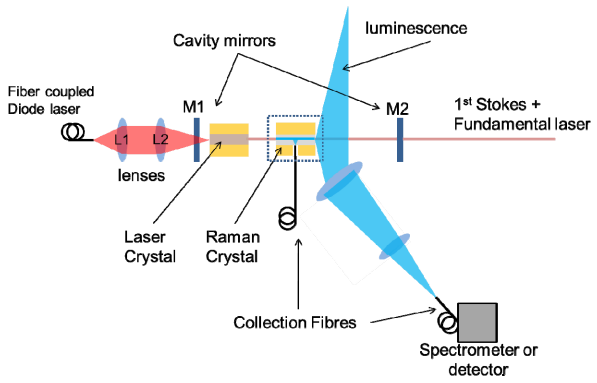

Fig. 2. Setup used for spectral measurements of blue emission. The Raman crystal was omitted for a self-Raman configuration.

Figure 3 shows blue emission spectra for the various crystals, recorded for a diode pump power of 15 W. Note the arbitrary units in all plots – there is no correspondence in the relative intensity of the signals from different crystals. It is possible to see strong similarities between the spectra for all the four crystals, despite the fact that two are vanadates and two are tungstates, and that two are intentionally doped with Nd^{3+} and two are undoped. There are even stronger similarities between tungstate based hosts and between vanadate based hosts. In addition, the high spectral resolution reveals substructure in the emission that can be compared to high resolution spectra found in the literature. We found that our blue spectra from Nd:YVO_4 was quite similar to that reported in [20] for YVO_4 doped with 1at.% Tm^{3+} and 8at.% Yb^{3+}, while that for KGW was almost identical to that reported in [21] for Tm:KGW. Specifically, we found our spectra for KGW had an overall width of 7 nm and peaks at 474 nm, 476 nm and 480 nm which closely matched those reported in [21] for Tm:KGW.

Qualitative observations were made about the intensity of the blue emission in different crystals for the same amount of diode pump power. Blue emission was weakest for $BaWO_4$ and strongest for KGW. In the case of the vanadates, the blue emission from one Nd:$GdVO_4$ crystal (supplied by Northrop Grumman) was several times stronger than the other crystals.

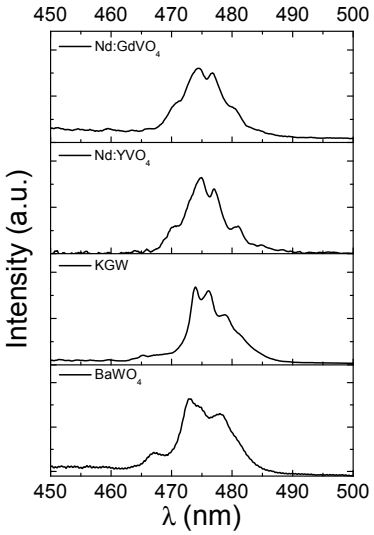

Fig. 3. Spectra of the blue emission for KGW, Nd:$GdVO_4$, $BaWO_4$, Nd:YVO_4

#203411 - $15.00 USD Received 24 Dec 2013; revised 22 Mar 2014; accepted 27 Mar 2014; published 1 Apr 2014

In order to measure the decay time of the blue emission, four Q-switched Raman lasers were built using different Raman active crystals. The lasers were similar to those described above, but with the addition of an acousto-optic Q-switch in the cavity (NEOS model 33027-25-2-1). A Nd:YAG crystal was used as the laser active medium in the case where separate Raman crystals (YVO_4, KGW and $BaWO_4$) were used. For Nd:$GdVO_4$ a self-Raman laser was built since there was no undoped $GdVO_4$ crystal available. Using a 50 mm lens to collect the blue emission from the Raman crystal and a 75 mm lens to image it into a photomultiplier tube (Hamamatsu R456), and filters to select only blue emission at 475nm, it was possible to measure luminescence decay times.

The decay curves for the Nd:$GdVO_4$, YVO_4, KGW and $BaWO_4$ are shown in Fig. 4. An exponential fit was used to extract decay times for each of them, which were then compared to lifetime values found in the literature for the same hosts doped with Tm^{3+}. These are summarised in Table 1. No data was available for Tm:$BaWO_4$. For KGW, we compared our measured decay time to lifetime values for a 0.1 at% Tm:KGW crystal [22]; the low Tm^{3+} concentration is good for comparing to our measurements, where any impurity Tm^{3+} concentration will be very low. For the vanadate crystals we compared to radiative lifetimes calculated for Tm^{3+} in $GdVO_4$ [23] and YVO_4 [24]; these represent an upper limit to the luminescence lifetime because they don't consider any parallel processes that may shorten the lifetime. It was found that the measured decay times were between 11% and 16% shorter than lifetimes taken from the literature, and given this level of agreement, it is safe to say that the measured decay time for the blue emission is consistent with the origin of that decay coming from the $^1G_4$ level of Tm^{3+} impurities. Finally, we note that Khodasevich *et al.* [16] measured the fall time (from 90% to 10%) of the blue emission in a Nd:KGW crystal, considering the intensity decay and found a value of 500 µs (which corresponds to 228 µs using the 1/e decay approximation). While experimental details in [16] are scant, their lifetime using the 1/e decay approximation is close to the literature value of 127 µs for Tm:KGW [22] and is consistent with a non-instantaneous processes like upconversion.

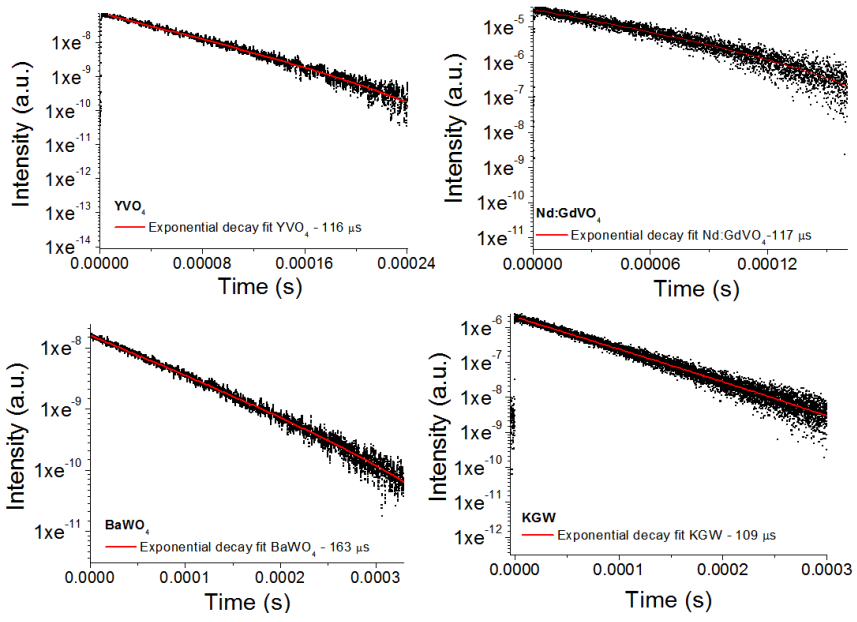

Fig. 4. Decay curves of the blue emission in Nd:$GdVO_4$, YVO_4, KGW and $BaWO_4$.

#203411 - $15.00 USD Received 24 Dec 2013; revised 22 Mar 2014; accepted 27 Mar 2014; published 1 Apr 2014

Table 1. Experimental blue luminescence lifetime and $Tm^{3+}(^1G_4)$ lifetimes from the literature for KGW, $BaWO_4$, $GdVO_4$ and YVO_4.

	Luminescence decay time – this work (μs)	$Tm^{3+}(^1G_4)$ lifetime – literature (μs)
KGW	109 ± 2	127 (0.1 at%) fluorescence lifetime [22]
$BaWO_4$	163 ± 2	-
Nd:$GdVO_4$	117 ± 2	140 radiative lifetime [23]
YVO_4	116 ± 2	131 radiative lifetime [24]

1.3 Analysis of visible emission

The blue band at 475 nm is by far the strongest emission from the Raman crystals when SRS is taking place, but it is not the only visible emission. The richest spectrum was found to come from Nd:$GdVO_4$. Figure 5(a) shows the spectrum of visible emission between 450 nm and 700 nm, measured for Nd:$GdVO_4$ above the threshold for SRS, and the luminescence excited from Nd:$GdVO_4$ (the resonator was blocked for this measurement). It is clear from the spectra in Fig. 5(a) that emissions around 525 nm, 550 nm and 600 nm are present above and below the SRS threshold, while the blue emission (475 nm) and the red emission around 650 nm only become strong above the SRS threshold. This suggests that the blue and red emissions do not arise from standard Nd^{3+} fluorescence. In the case of KGW, far weaker blue luminescence (by at least an order of magnitude) was observed below SRS threshold, and this was also noted in [16].

(a) (b)

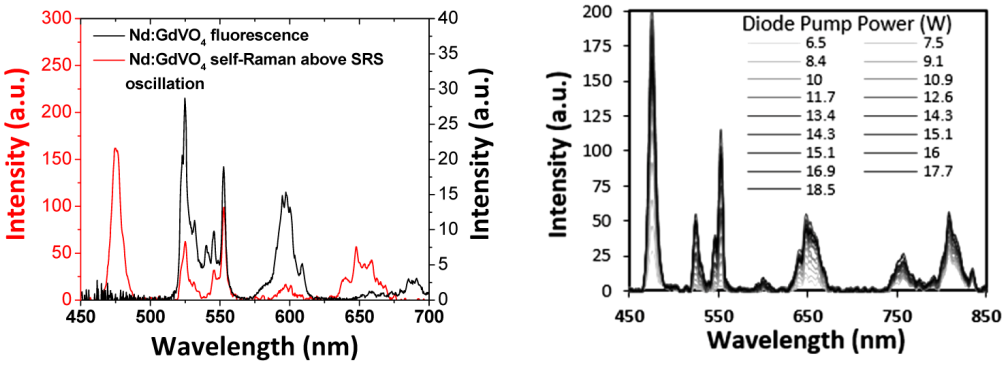

Fig. 5. (a) Emission spectra from Nd:$GdVO_4$ crystal above the SRS threshold, and fluorescence only (resonator blocked). (b) Emission spectra as a function of diode pump power.

Emission spectra were also collected for various diode pump powers above the SRS threshold. These spectra are shown in Fig. 5(b). The powers measured after the output coupler at diode (880 nm), fundamental (1063 nm) and Stokes (1173 nm) wavelengths were also collected. It was not possible to find clear (uni-variate) correspondences between variables (e.g. peak luminescence intensities and infrared powers). For this reason, we chose to adopt a multivariate approach to analyzing this data. The data was imported into The Unscrambler 10.2 (Camo Software), a statistical analysis program primarily designed for spectroscopic analysis, and the spectra were pre-processed using 5 point Savitsky-Golay smoothing and to remove the baseline. All data were mean centred and scaled to account for both the relatively low intensity luminescence and the high intensity laser output.

#203411 - $15.00 USD Received 24 Dec 2013; revised 22 Mar 2014; accepted 27 Mar 2014; published 1 Apr 2014

The Unscrambler performs eigenvector decomposition of the data set to reduce dimensionality, generating new orthogonal variables (principal components) which correspond to maximum variability in the data set [25]. The first two variables generated in this case are the principal components (PC1 and PC2) shown in Fig. 6, and together they account for 99% of the variance in the data.

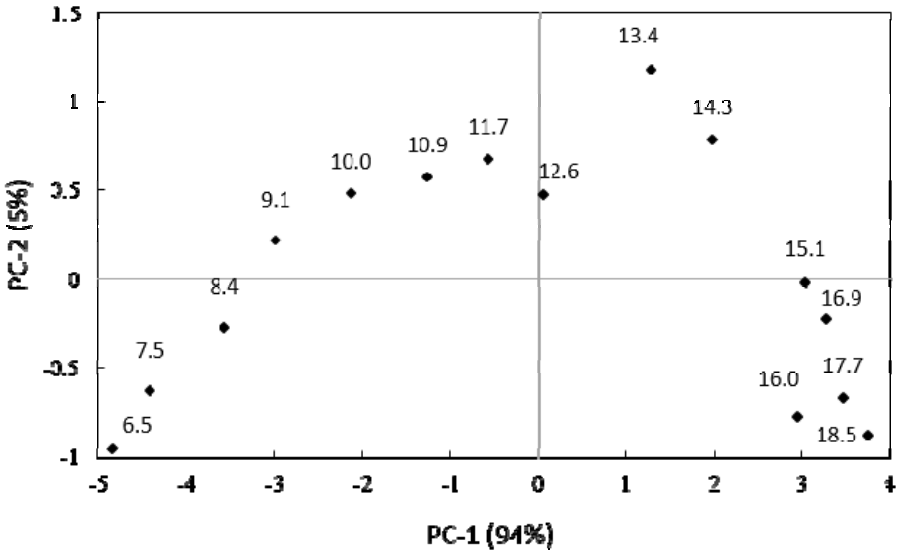

Fig. 6. PCA scores plot. Point labels correspond to diode pump power (W). PC-1 explains 94% of data variance, PC-2 explains 5%.

Principal component 1 (PC1) primarily represents the increase of light emission with pump power (the factor producing the greatest variability in the data set). Different behaviours are observed for the 6.5-12.6 W power range and the 13.4-18.5 W power range (this latter range corresponds to a roll-off in laser output). Component 2 (PC2) increases with increasing diode pump power and then declines as the pump power increases further. Figure 7 shows the loadings plot corresponding to Fig. 6. The loadings represent the correlation between the scores and the principal components. The emissions at 475 nm and 648 nm cluster together and are well separated from the green emissions (525 nm, 546 nm and 553 nm). This indicates strong correlation between the red and blue emissions, which is consistent with these lines emanating from the same upper energy level. The clustering of the green lines is also consistent with the suggestion by Khodasevich that they arise from Er^{3+} impurities [16].

#203411 - $15.00 USD Received 24 Dec 2013; revised 22 Mar 2014; accepted 27 Mar 2014; published 1 Apr 2014

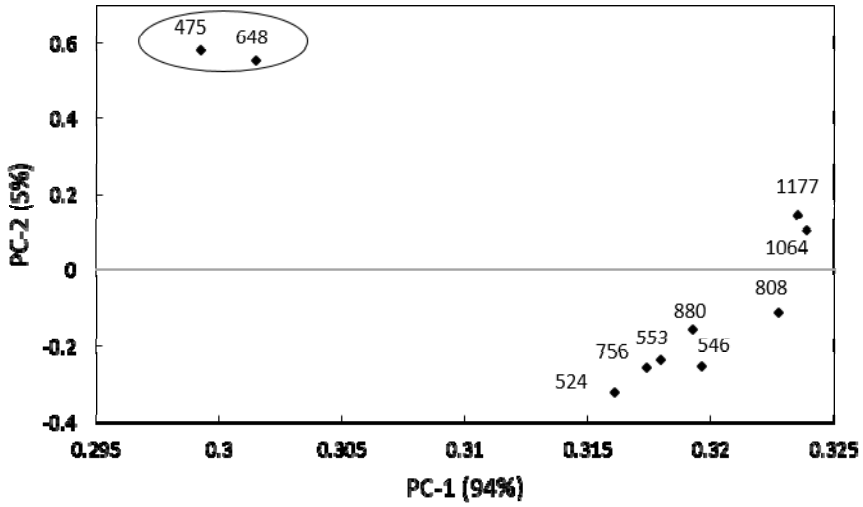

Fig. 7. PCA loadings plot. Point labels correspond to peak wavelengths (nm).

1.4 Measurement of impurity ion concentrations in Raman-active crystals

Inductively-coupled plasma mass spectrometry is a well-known method to quantify the elements contained in a specific material. In the 7500 ICP-MS (Agilent), used for this work, a laser is used to ablate material from crystal samples. The ablated material goes to the plasma torch of the ICP-MS where it is ionized and quantified by a mass spectrometer.

We have measured the concentration of trace elements in several Raman-active crystals investigated here to verify the presence of Tm^{3+} in two different Nd:$GdVO_4$ crystals from Northrop Grumman (NG) and Castech, and Tm^{3+} and Nd^{3+} in undoped KGW and $BaWO_4$ crystals. We also measured the concentration of Tm ions in $LiIO_3$ and $LiNbO_3$, two crystals in which we observed an absence of blue emission, and found the Tm concentration to be below the minimum detectable limit, ie <0.0069ppm for $LiNbO_3$ (HC Photonics) and <0.0071ppm for $LiIO_3$. The concentrations averaged for the two locations measured are shown in Table 2. The quoted uncertainties relate to the difference found in the two measurements.

Table 2. Concentration of Nd^{3+} and Tm^{3+} found in the in the Raman crystals studied.

	Concentration in ppm weight ± 10%			
	Nd:$GdVO_4$ (Castech)	**Nd:$GdVO_4$ (NG)**	**KGW**	**$BaWO_4$**
Tm^{3+}	0.069	0.279	0.090	0.0085
Nd^{3+}	1759.48	1417.42	0.343	0.035

In order to cross-check the measured concentration values, we have calculated the expected ppm values using the stoichiometric distribution for each crystal, and setting one of the main host elements to calibrate the others (e.g. V for the $GdVO_4$, W for the KGW and Ba for the $BaWO_4$). We then checked the ppm concentration of the other main contents, and they were well matched to the calculated ones, with only a small error (5%).

As noted above, at similar pump levels, the blue emission in the Nd:$GdVO_4$ crystal from NG was markedly stronger than for the crystal from Castech. This corresponds well with the measured Tm^{3+} concentration being four times higher for the NG crystal. Similarly, blue emission from KGW was much stronger than for $BaWO_4$, and this corresponds to a much higher Tm^{3+} concentration in the KGW. While the concentrations found are small, it is possible to have an intense blue emission if the excitation rates of Tm^{3+} are high.

#203411 - $15.00 USD Received 24 Dec 2013; revised 22 Mar 2014; accepted 27 Mar 2014; published 1 Apr 2014

Part 2: Proposed origin of the blue emission

Based on the spectroscopic investigation detailed above, we consider it most likely that the blue luminescence originates from the $^1G_4$ to $^3H_6$ transition in Tm^{3+}, which is present as an impurity in the crystals we have studied. A large body of evidence supports this conclusion. Firstly there are the spectral similarities between the blue emission from various crystals, and by their Tm^{3+}-doped counterparts, and the similarities between measured lifetimes and those reported in the literature. Second the similar behaviours of the blue and red emission that are apparent from spectra taken above and below threshold, and also indicated by multi-variate analysis of the visible and near-IR emission spectra, are consistent with both blue and red transitions emanating from the same $Tm^{3+}(^1G_4)$ level. Finally, the ICP-MS measurements prove the presence of Tm^{3+} impurities in all the hosts studied here, with higher Tm^{3+} concentrations determined in crystals with higher levels of blue luminescence.

We can now proceed to propose the sequential absorption mechanism that raises the Tm^{3+} ions to the $^1G_4$ level, which then emits in the blue. It involves three steps, as shown in Fig. 8. First, a Tm^{3+} ion in the ground state ($^3H_6$) is excited to $^3H_5$ by the absorption of a 1st Stokes photon, which decays rapidly and non-radiatively to populate the $^3F_4$ level. Next, the absorption of another 1st Stokes photon or a fundamental photon populates the $^3F_3$ or $^3F_2$ levels respectively, which rapidly decay non-radiative decay to populate the $^3H_4$ level. Finally, another Stokes photon is absorbed, thus populating the $^1G_4$ level.

Table 3 lists the fundamental and first Stokes photon energies, and the energy separation of the levels involved, as sourced from the Stark levels given in [26] for Tm:YVO_4 at 300K. It can be seen that the Stokes photon energy is well-matched to the transitions labeled S1, S2, S3, while the fundamental photon energy is well-matched to the transition labeled F1. Two multiphonon transitions are denoted by H1 and H2. We speculate that the absorption steps could be assisted to some extent by the phonon field built up by the SRS process, as this could explain the typical lack of blue fluorescence in non-Raman-active laser crystals. It is also worth noting that this same 3-step sequential upconversion scheme has been used for efficient excitation of blue Tm-doped upconversion fibre lasers. For example in [27], 1.6 W of pump power at 1123 nm gave rise to 230 mW blue laser output at 481 nm, and the optimum pump wavelength was identified as 1140 nm, for that Tm:ZBLAN host.

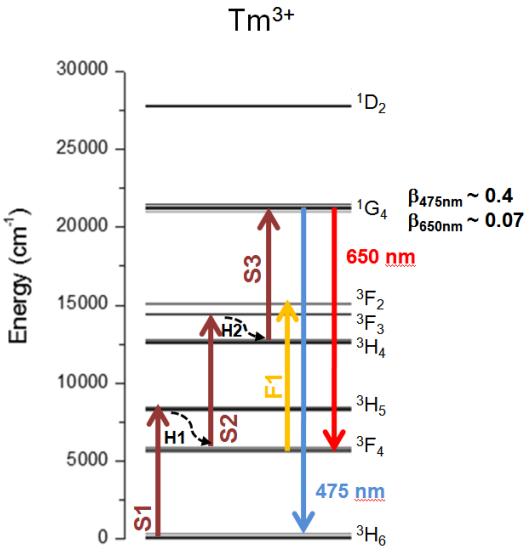

Fig. 8. Energy level diagram for Tm:YVO_4 showing blue upconversion steps [26].

#203411 - $15.00 USD Received 24 Dec 2013; revised 22 Mar 2014; accepted 27 Mar 2014; published 1 Apr 2014

Table 3. Transitions, photon and phonon energies for the Tm:YVO_4 system.

	Energy (cm^{-1})								
	1st Stokes supported transitions			Fundamental supported transition	Multiphonon supported transitions		1064 nm	1176 nm	Highest phonon energy
	S1	S2	S3	F1	H1	H2			
Min	7872	8532	8164	9128	2325	1637	9398	8503	890
Max	8491	8925	8936	9597	2941	1952			

Part 3: The implications of blue fluorescence for Raman laser performance

3.1 Power measurement of blue emission

To determine if the excitation processes resulting in blue emission have any significant impact on the operation of Raman lasers, it is necessary to make an accurate absolute measurement of the power emitted on the observed blue band. For this, we used an integrating sphere (Labsphere) in the setup displayed in Fig. 9. The Raman laser we constructed for this purpose used a Nd:YLF crystal as the active medium and KGW as the Raman active medium. The Stokes wavelength in this case was 1163 nm. This combination of crystals was chosen because the KGW (oriented for the 901 cm^{-1} shift) exhibited strong blue emission, and the Nd:YLF was used because its weak thermal lens enabled a long cavity to be made which would accommodate the integrating sphere, which had a diameter of 9.5 cm. The laser was similar to that described in section 1.2, however the longer cavity length resulted in a resonator mode less well matched to the pump mode, and as a consequence, the laser did not operate so efficiently as for shorter cavities. However this was not considered important in this case, given the complexity of the measurement. Measurement of the blue emission power was made for the case where the absorbed pump power was 15 W, the Stokes power was 470 mW, and the residual fundamental power was 850 mW.

The integrating sphere was positioned carefully in the laser resonator, and the 25 mm long KGW crystal was inserted into the sphere on a metal platform wrapped in white teflon tape to minimize absorption and the blue power incident on the silicon detector at the exit port of the sphere was measured. A photopic filter was placed in front of the detector, in order to exclude any infrared emission. Considerable attention was paid to calibrating the collection efficiency of the arrangement, which was accomplished with the aid of a green laser pointer of known output power. We measured a total blue emission power of P_{blue} = 19 mW ± 2.8 mW.

#203411 - $15.00 USD Received 24 Dec 2013; revised 22 Mar 2014; accepted 27 Mar 2014; published 1 Apr 2014

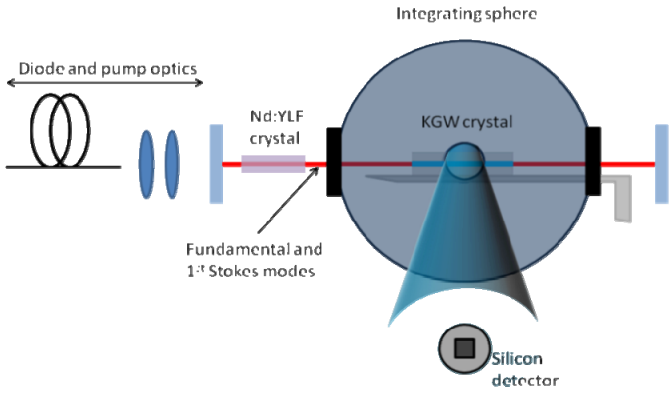

Fig. 9. Laser cavity with the integrating sphere used to measure the blue emission power.

3.2 Implications of blue emission for laser efficiency

Intracavity Raman lasers are characterized by relatively low gain, and to achieve good performance it is absolutely critical to minimize resonator losses. The mirror reflectivities used here are very high, so that the resonator losses are typically dominated by bulk crystal losses associated with scattering and absorption [28]. Therefore it is reasonable to question whether the blue emission presents a significant loss to the intracavity Stokes optical field.

Here we consider the worst case scenario, which is the use of three Stokes photons to reach the $Tm^{3+}(^1G_4)$ level. We also recognize that not every Tm^{3+} ion in the $^1G_4$ level will decay by emitting a blue photon and so, the branching ratio (β) of the $^1G_4$ level and the quantum efficiency (η_{qe}), have to be taken in account. The branching ratio value (0.4) is found in the literature [24], while the quantum efficiency is calculated from the ratio of the measured fluorescence lifetime (τ_f) to the radiative lifetime (τ_r). In this case we used the fluorescence lifetime found in the literature for a low Tm^{3+} doping concentration (0.1at%), which is expected to be close to the radiative lifetime. Based on the lifetime values described in the previous section, the quantum efficiency is calculated to be 0.86.

For a measured blue power P_{blue}, we find the number of blue photons emitted is $N_{blue} = P_{blue}/h\nu_{blue}$. The number of Tm^{3+} ($^1G_4$) ions excited to generate P_{blue} can be calculated by

$$N_{Tm(1G4)} = \frac{N_{blue}}{\eta_{qe} \cdot \beta} \tag{1}$$

Now we assume that three Stokes photons were consumed for each $^1G_4$ level that was excited, and find the power extracted from the Stokes field is given by

$$P_{Stokes} = 3 \cdot h\nu_S \cdot N_{Tm(1G4)} \tag{2}$$

where h is the Planck constant, ν_s is the Stokes frequency. For the measured value of P_{blue} of 19 mW, we find that 68 mW of Stokes power are extracted from the intracavity Stokes field.

Based on the coupling mirror transmission of 0.2% and the measured output power the intracavity Stokes field is estimated to be approximately 230 W. The 68 mW represents a loss of about 0.029% for the Stokes field. For the case where only two Stokes photons and one fundamental photon are involved in the process, this loss will be somewhat lower.

If we were able to prevent the processes leading to blue emission and the associated 0.029% loss (by using a KGW crystal with zero Tm^{3+} impurity) we would in principle be able to increase the output coupling by an equivalent 0.029% while maintaining the same intracavity optical powers, and so extract an additional 68 mW of Stokes output power, increasing the Stokes output power by 15% to 538 mW.

#203411 - $15.00 USD Received 24 Dec 2013; revised 22 Mar 2014; accepted 27 Mar 2014; published 1 Apr 2014

The extent to which the efficiency of other Raman lasers may be impacted by the processes leading to blue fluorescence depend on the power of the blue emission and the output coupling for the Stokes field. However it is reasonable to conclude that crystals containing high levels of Tm^{3+} impurity will experience commensurately higher losses. We note in this context that the geometric constraints of the integrating sphere made it impractical to measure the absolute power of blue emission for the self-Raman laser crystals.

3.3 Implications of blue emission for thermal loading of Raman-active crystals

It has been noted on several occasions [29, 30] that the thermal lensing in CW intracavity Raman lasers is somewhat stronger than anticipated on the basis of estimated thermal loads due to pump heating and Raman heating. In [30], the thermal lens in an intracavity Nd:$GdVO_4$ Raman laser was measured interferometrically, and the slope of the thermal lens power was found to approximately double above the threshold for SRS; it was suggested that this might be linked to the strong blue emission observed in that system. Here we consider the possibility that the excitation processes leading to blue emission might be contributing to the thermal load in a Raman-active crystal, based on the measured blue power of 19 mW from KGW.

In order to find the thermal power added due to the blue fluorescence, we first consider the three sequential absorption steps for excitation of the $Tm^{3+}(^1G4)$ level. As shown in Fig. 8, the energy of 3 Stokes photons exceeds the energy level of Tm ($^1G_4$), the difference being the energy of the two nonradiative decays labelled H1 and H2 in Fig. 8. This gives a first contribution to the thermal load associated with the blue fluorescence.

$$P_{heat\ blue\,1} = \left(3 \cdot h\nu_S - h\nu_{blue}\right) \cdot N_{Tm(1G4)} = 12.44\ \text{mW} \tag{3}$$

where $N_{Tm(1G4)}$ is from Eq. (2).

Now we consider the various decay channels for $Tm^{3+}(^1G_4)$ ions. Those that decay radiatively to the ground state by emitting a blue photon contribute no thermal load. Those 14% that decay nonradiatively are assumed to contribute fully to the thermal load, and so

$$P_{heat\ blue\,2} = P_{Stokes} \cdot \left(1 - \eta_{qe}\right) = 9.47\ \text{mW} \tag{4}$$

For the other 60% of Tm-$^1G_4$ ions that decay radiatively eg at 650 nm or 800 nm to levels other than the ground state, we estimate that ~1/3 of the energy is deposited as heat.

$$P_{heat\ blue\,3} = \frac{P_{blue} \cdot \dfrac{0.6}{0.4}}{3} = 9.5\ \text{mW} \tag{5}$$

where P_{blue} is the blue power measured with the integrating sphere setup.

Summing the different contributions we find that the total heat deposited in the KGW Raman crystal by the processes leading to the blue emission is $P_{heat\ blue}$~31 mW. The main uncertainty in this estimate is whether all the blue photons emitted from $Tm^{3+}(^1G_4)$ are detected, ie that there is no reabsorption of the blue emission. Given the low Tm^{3+} and Nd^{3+} concentrations, at least in KGW, this is a reasonable assumption.

Next we consider the Raman heating, so that the two heat loads can be compared. For every Stokes photon generated, a small amount of heat ($h\nu_f - h\nu_s$) is deposited in the Raman crystal. To determine the Stokes power generated we must consider the Stokes output power plus the Stokes photons lost as a result of passive cavity losses and blue generation. Thus the Raman heating in the Raman crystal is given by

$$P_{heat\ Raman} = \frac{\left(h\nu_f - h\nu_s\right) \cdot P_{Stokes}^{out} \cdot \left(T_{oc} + L_{passive} + L_{blue}\right)}{T_{oc}} \tag{6}$$

#203411 - $15.00 USD Received 24 Dec 2013; revised 22 Mar 2014; accepted 27 Mar 2014; published 1 Apr 2014

In the present example, where the passive round trip cavity losses are estimated to be ~0.5%, we then estimate that the generated Stokes power is 3.65 times higher than the Stokes output power of 470 mW, ie it is 1.72 W. From Eq. (6), the thermal load associated with Raman heating can be calculated to be ~178 mW, and the total heat load ($P_{heat\ Raman} + P_{heat\ blue}$) is 209 mW.

If we were able to prevent the blue emission in this particular laser, for example by using a KGW crystal with no Tm^{3+} impurity ions, and we increased the output coupling by 0.029% to maintain the same intracavity Stokes field, then the total heat load would be reduced by 17%, to the Raman heating component only (178 mW). This is a 17% reduction in heat load, and would be accompanied by the 15% increase in output power discussed in the previous section. Lowering the pump power to keep the Stokes output power at 470 mW would result in a total heat load of 151 mW, 25% less than for the same laser at the same output power. We can also see that in the event that the round trip losses were in fact lower than the estimated 0.5%, then the additional thermal load due to the blue fluorescence would become even more significant. We note that these estimates of the thermal load are very dependent on the round trip loss values, which are notoriously difficult to measure.

The analysis above suggests that for the KGW Raman laser considered here, the blue fluorescence leads to an additional thermal load of 17%. The extent to which blue fluorescence might impact thermal loading of other Raman lasers will depend on the power of the blue emission, and the total cavity losses for the Stokes field. For the case of self-Raman lasers such as in [30], we anticipate the resonator round trip losses would be lower than those estimated here, however heating associated with the quantum defect between the diode pump and fundamental pump photon energies will dominate Raman heating. For 15 W absorbed diode pump power, pump heating would amount to around 3.7 W. Thus it appears quite unlikely, that the thermal loading associated with blue fluorescence (31 mW in the case of the KGW Raman laser) would make a substantial contribution to the overall thermal load in a self-Raman laser.

Conclusion

The phenomenon of blue emission from a variety of Raman-active crystals has been investigated in detail. Various spectroscopic methods were used to measure the spectral characteristics of the blue emission, its lifetime, and power-dependence, while ICPMS was used to determine the concentration of Tm^{3+} ions. This investigation leads us to attribute the origin of the phenomenon to fluorescence from Tm^{3+} ($^1G_4$) impurity ions which are excited via sequential upconversion.

For the specific case of a Nd:YLF/KGW Raman laser, in which the KGW crystal contained Tm^{3+} impurity ions at 0.09 ppm, we measured the blue fluorescence power to be around 19 mW. Loss to the first-Stokes optical field associated with the proposed excitation mechanism was estimated to be 68 mW or 0.029%. We further found that if the processes leading to blue fluorescence could be eliminated, the laser efficiency could be increased by 15% and thermal loading in the KGW crystal reduced by 17%.

We conclude generally that high levels of Tm^{3+} impurity in tungstate and vanadate Raman crystals will result in significantly inferior Raman laser performance; conversely crystals with low levels of Tm^{3+} impurity will give best performance.

Acknowledgments

Jonas Jakutis Neto gratefully acknowledges the award of a CAPES scholarship (Proc nº 5381/09-6) and IMQRS scholar from Macquarie University. We gratefully acknowledge our colleagues Prof. Jiyang Wang and Huaijin Zhang from the State Key Laboratory of Crystal Materials, Shandong University, China who provided the Barium tungstate crystal used for this work.

#203411 - $15.00 USD Received 24 Dec 2013; revised 22 Mar 2014; accepted 27 Mar 2014; published 1 Apr 2014